The Good, the Neutral, and the Positive: Buffer Identity Impacts CO_2 Reduction Activity by Nickel(II) Cyclam

Camille R. Schneider, Luke C. Lewis, and Hannah S. Shafaat

Electronic Supporting Information
Table of Contents

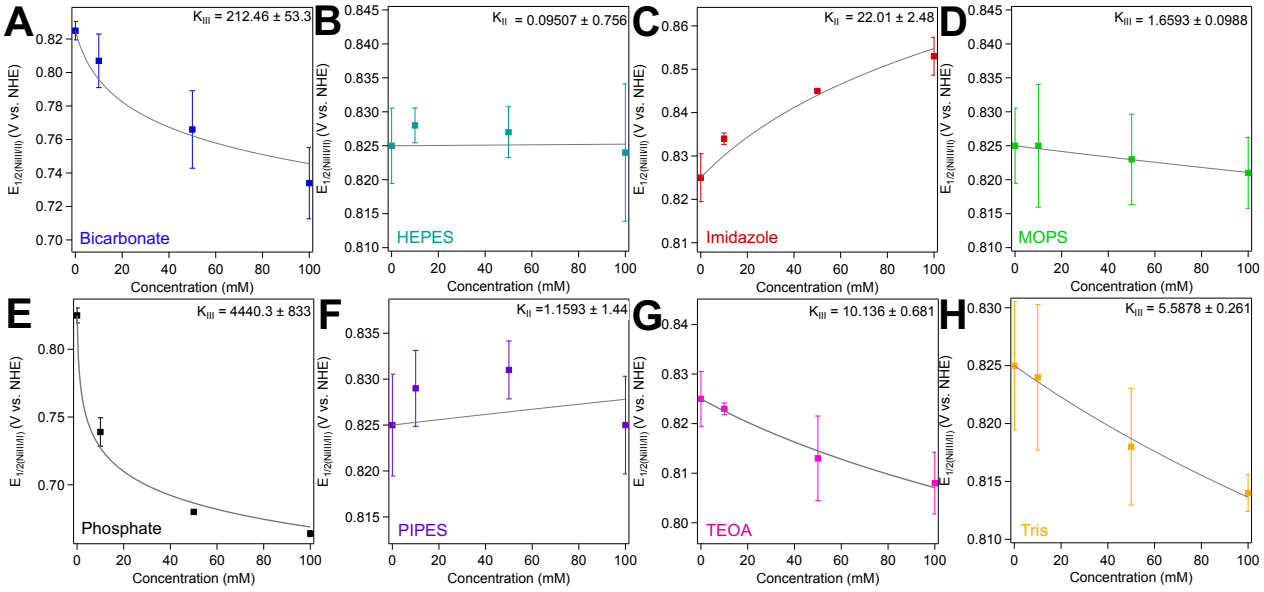

Figure S1. Midpoint potentials ($E_{1/2}$) for [$Ni^{III/II}$(cyclam)] as a function of buffer concentration (0, 10, 50, and 100 mM). Specific buffer used in each experiment is noted in the panel. All samples contained 100 µM [Ni(cyclam)]$^{2+}$, 100 mM KCl, and indicated concentration of buffer at a final pH of 7.0. CVs were conducted under an inert atmosphere at a scan rate of 10 mV/s using a glassy carbon working electrode, Ag/AgCl reference electrode, and a Pt wire counter electrode. Reduction potentials are reported against the normal hydrogen electrode by the addition of +198 mV to the experimentally determined values. The K_N for each buffer was determined using Equation 4 of the main text. K_{III} represents preferential binding to the Ni^{III} state of [Ni(cyclam)], while K_{II} represents preferential binding to the Ni^{II} state. Best-fits to Equation 4 were determined using Igor Pro 8.

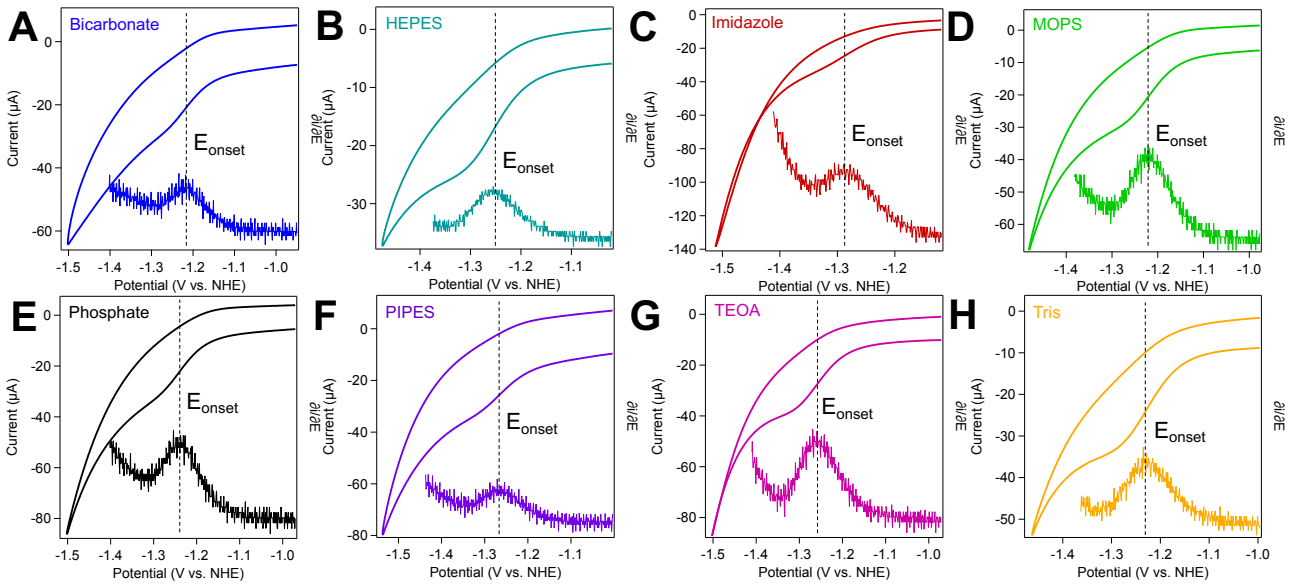

Figure S2. *E_{onset}* determination for CO_2 reduction by [Ni(cyclam)] in each buffer. Specific buffer used for each experiment is noted in the panel. The maximum of the first derivative of the cathodic scan was used to determine the onset potential of catalysis for each buffer which is indicated as a dotted line in each panel. All reactions contained 100 μM $[Ni(cyclam)]^{2+}$, 100 mM KCl, and 100 mM buffer at a final pH of 7.0. CVs were conducted under a CO_2-saturating atmosphere at a scan rate of 1 V/s using a glassy carbon working electrode, Ag/AgCl reference electrode, and a Pt wire counter electrode. Reduction potentials are reported against the normal hydrogen electrode by the addition of +198 mV to the experimentally determined values. Data were analyzed using Igor Pro 8.

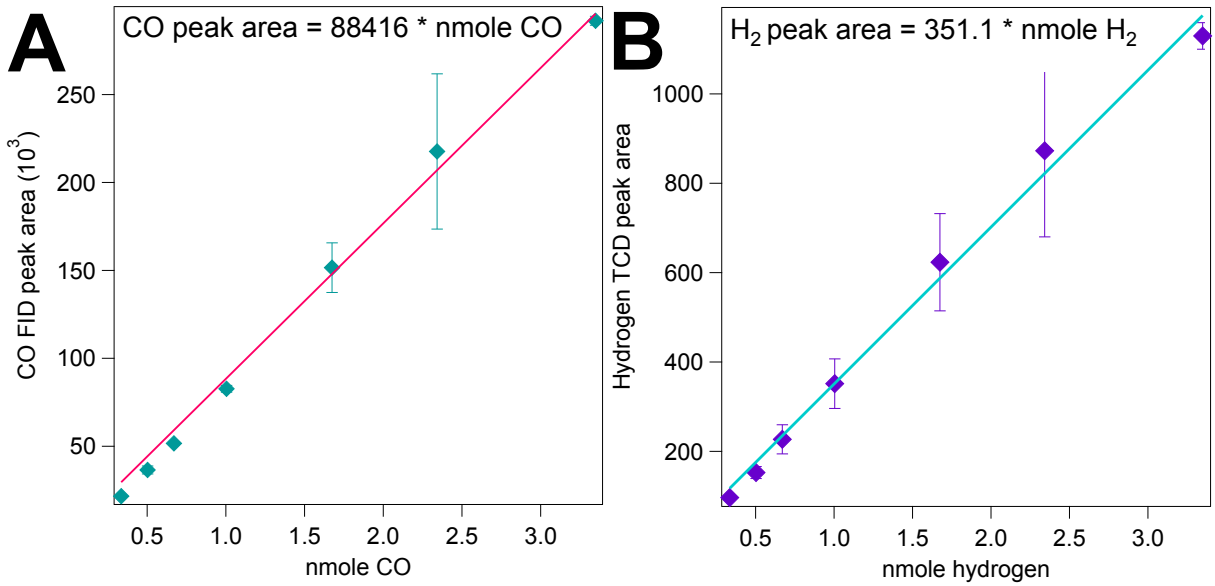

Figure S3. Gas chromatography calibration curves and equations for (**A**) carbon monoxide and (**B**) hydrogen.

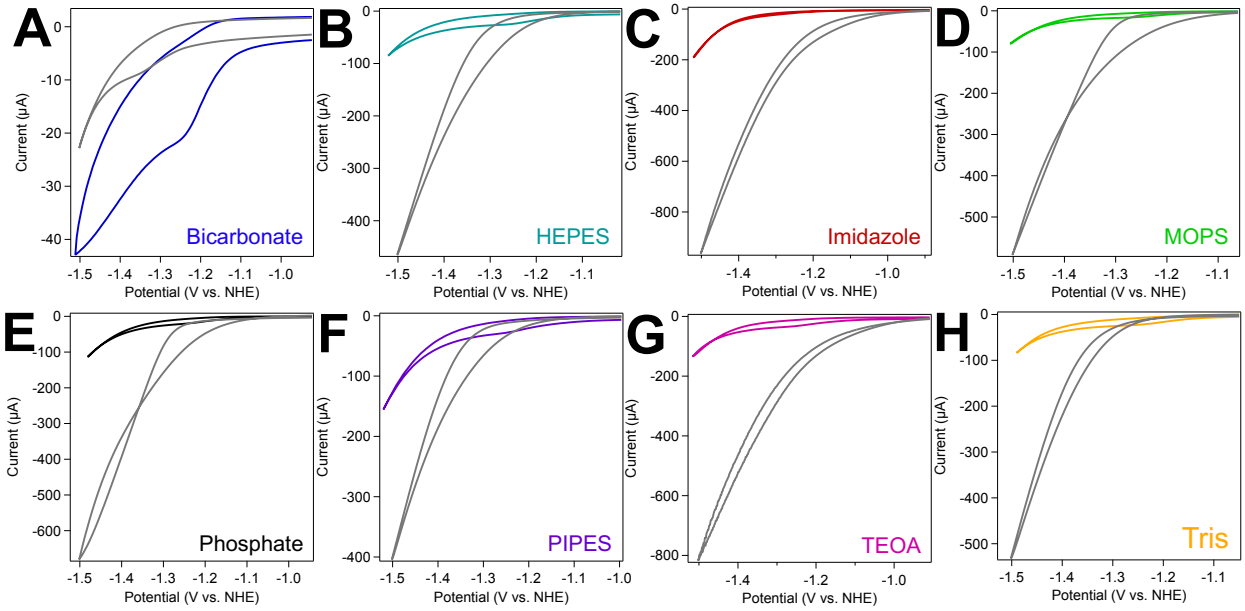

Figure S4. Cyclic voltammograms at negative potentials of $[Ni(cyclam)]^{2+}$ under an inert Ar atmosphere (grey) compared to a CO_2-saturated atmosphere (colored and labeled as indicated in panel). All experiments contained 100 μM $[Ni(cyclam)]^{2+}$, 100 mM KCl, and 100 mM buffer at a final pH of 7.0. CVs were conducted at a scan rate of 100 mV/s using a glassy carbon working electrode, Ag/AgCl reference electrode, and a Pt wire counter electrode. Reduction potentials were reported against the normal hydrogen electrode by the addition of +198 mV to the experimentally determined values.

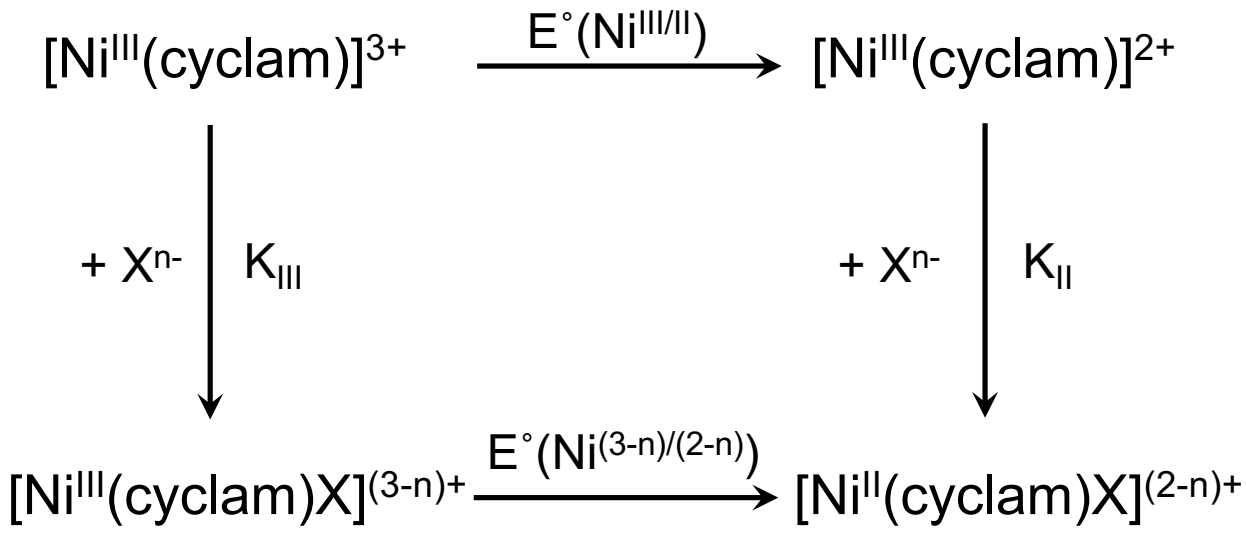

Figure S5. Square scheme used to derive the binding constant K_N. X denotes the buffer.

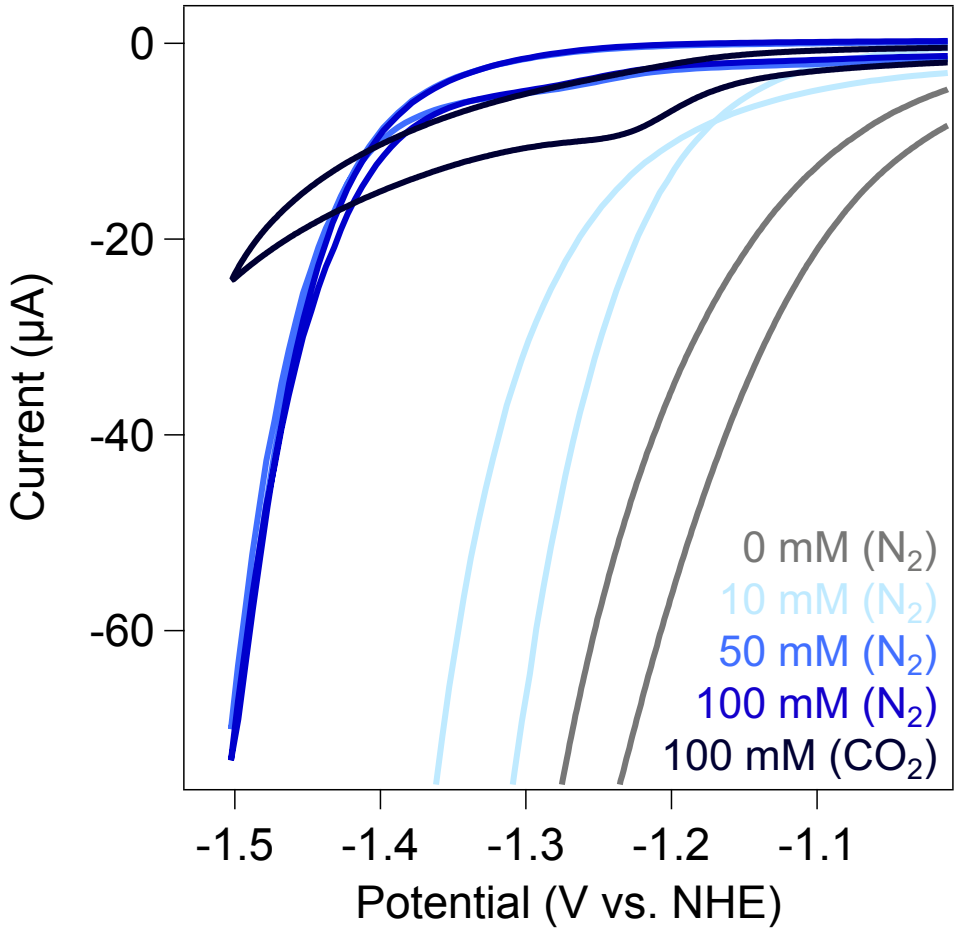

Figure S6. Cyclic voltammograms of $[Ni(cyclam)]^{2+}$ in increasing concentrations of sodium bicarbonate buffer. All measurements were conducted at a scan rate of 25 mV/s and contained 100 µM $[Ni(cyclam)]^{2+}$. The buffer concentration, pH adjusted to pH 7.0, is as indicated in figure with the atmosphere denoted in parentheses. CVs were conducted using a glassy carbon working electrode, Ag/AgCl reference electrode, and a Pt wire counter electrode. Reduction potentials were reported against the normal hydrogen electrode by the addition of +198 mV to the experimentally determined values.

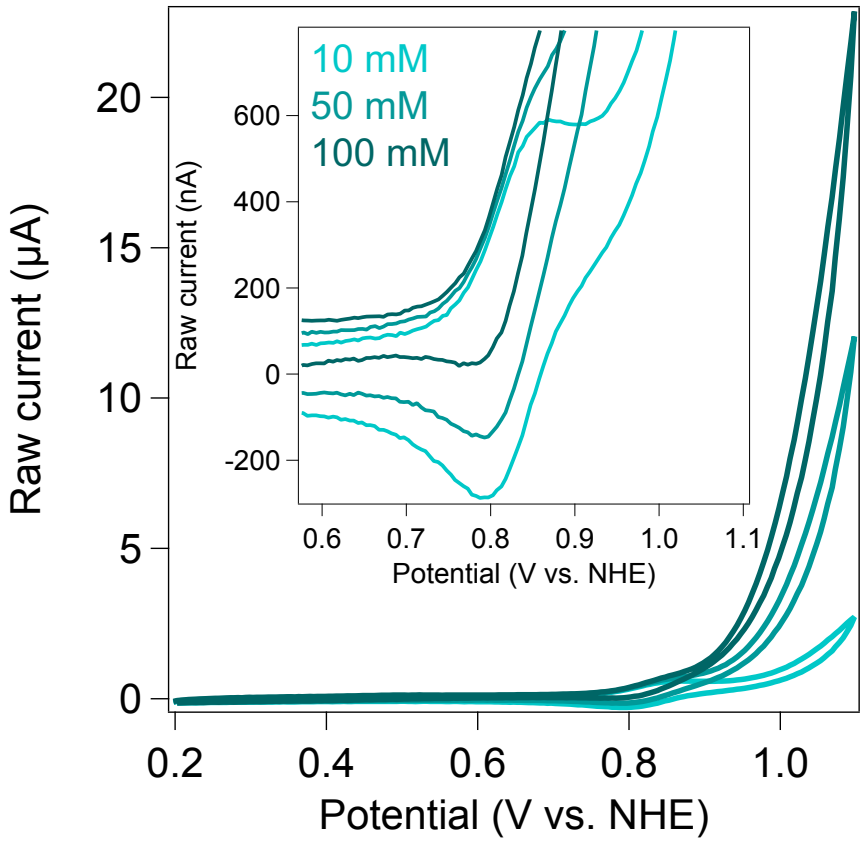

Figure S7. Cyclic voltammograms of $[Ni(cyclam)]^{2+}$ in increasing concentrations of HEPES buffer under an inert atmosphere. All samples were collected at a scan rate of 10 mV/s and contained 100 µM $[Ni(cyclam)]^{2+}$ and 100 mM KCl in HEPES buffer, pH 7.0, at the concentrations indicated in the figure. CVs were conducted using a glassy carbon working electrode, Ag/AgCl reference electrode, and a Pt wire counter electrode. Reduction potentials were reported against the normal hydrogen electrode by the addition of +198 mV to the experimentally determined values.

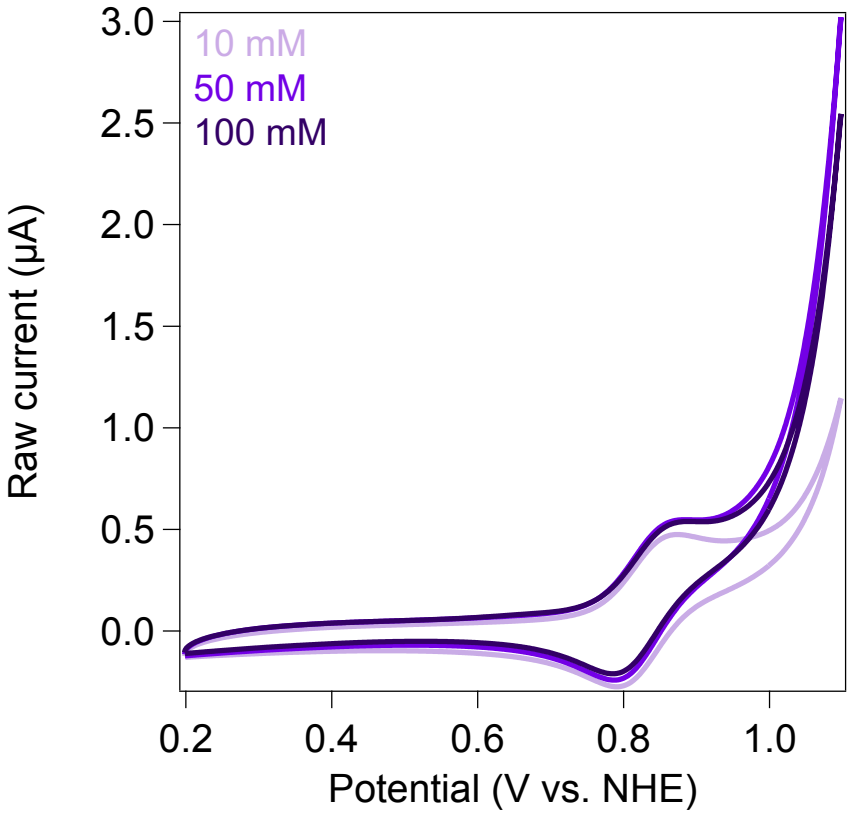

Figure S8. Cyclic voltammograms of $[Ni(cyclam)]^{2+}$ in increasing concentrations of PIPES buffer under an inert atmosphere. All samples were collected at a scan rate of 10 mV/s and contained 100 µM $[Ni(cyclam)]^{2+}$ and 100 mM KCl in PIPES buffer, pH 7.0, at the concentrations indicated in the figure. CVs were conducted using a glassy carbon working electrode, Ag/AgCl reference electrode, and a Pt wire counter electrode. Reduction potentials were reported against the normal hydrogen electrode by the addition of +198 mV to the experimentally determined values.

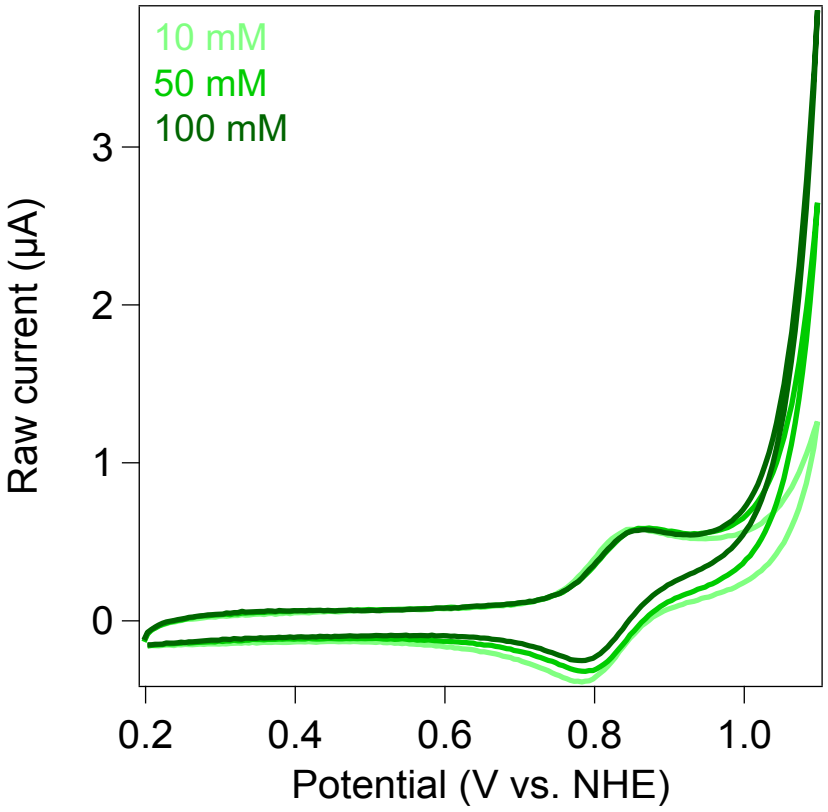

Figure S9. Cyclic voltammograms of $[Ni(cyclam)]^{2+}$ in increasing concentrations of MOPS buffer under an inert atmosphere. All samples were collected at a scan rate of 10 mV/s and contained 100 µM $[Ni(cyclam)]^{2+}$ and 100 mM KCl in MOPS buffer, pH 7.0, at the concentrations indicated in the figure. CVs were conducted using a glassy carbon working electrode, Ag/AgCl reference electrode, and a Pt wire counter electrode. Reduction potentials were reported against the normal hydrogen electrode by the addition of +198 mV to the experimentally determined values.

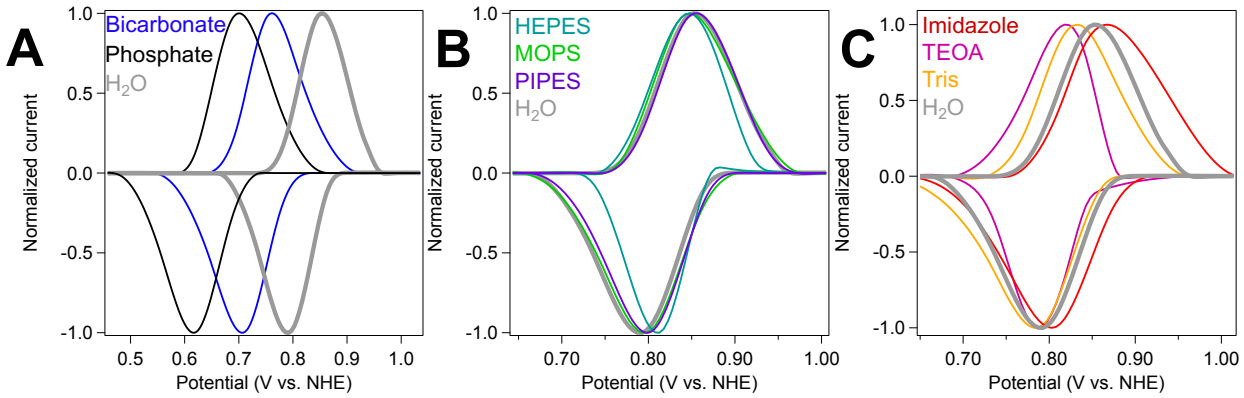

Figure S10. Baseline corrected and normalized data under an inert atmosphere. All reactions contained 100 µM $[Ni(cyclam)]^{2+}$, 100 mM KCl, and 100 mM buffer at a final pH of 7.0. Specific buffer used is indicated in the figure. CVs were conducted at a scan rate of 10 mV/s using a glassy carbon working electrode, Ag/AgCl reference electrode, and a Pt wire counter electrode. Reduction potentials were reported against the normal hydrogen electrode by the addition of +198 mV to the experimentally determined values. CVs were baseline-corrected in QSOAS and normalized using Igor Pro 8.

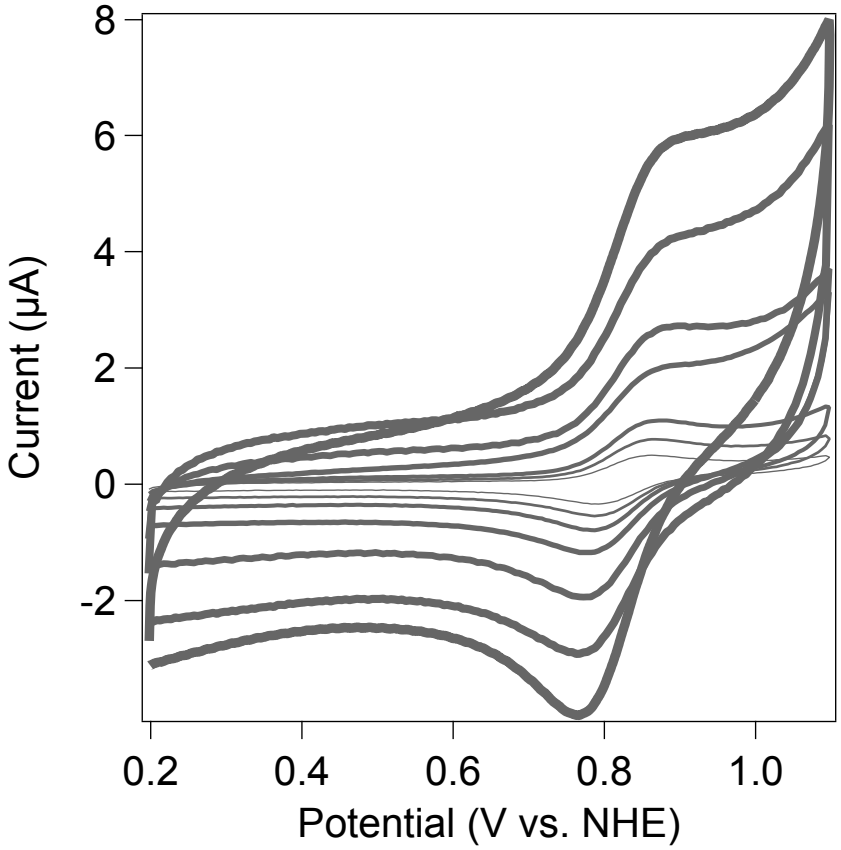

Figure S11. Cyclic voltammograms of $[Ni(cyclam)]^{2+}$ in water under an inert atmosphere at varying scan rates. Samples were collected at the following scan rates as depicted by increased line thickness: 10 mV/s, 25 mV/s, 50 mV/s, 100 mV/s, 250 mV/s, 500 mV/s, and 1 V/s. All samples contained 100 μM $[Ni(cyclam)]^{2+}$ and 100 mM KCl in pH-adjusted, unbuffered water, pH 7.0. CVs were conducted using a glassy carbon working electrode, Ag/AgCl reference electrode, and a Pt wire counter electrode. Reduction potentials were reported against the normal hydrogen electrode by the addition of +198 mV to the experimentally determined values.

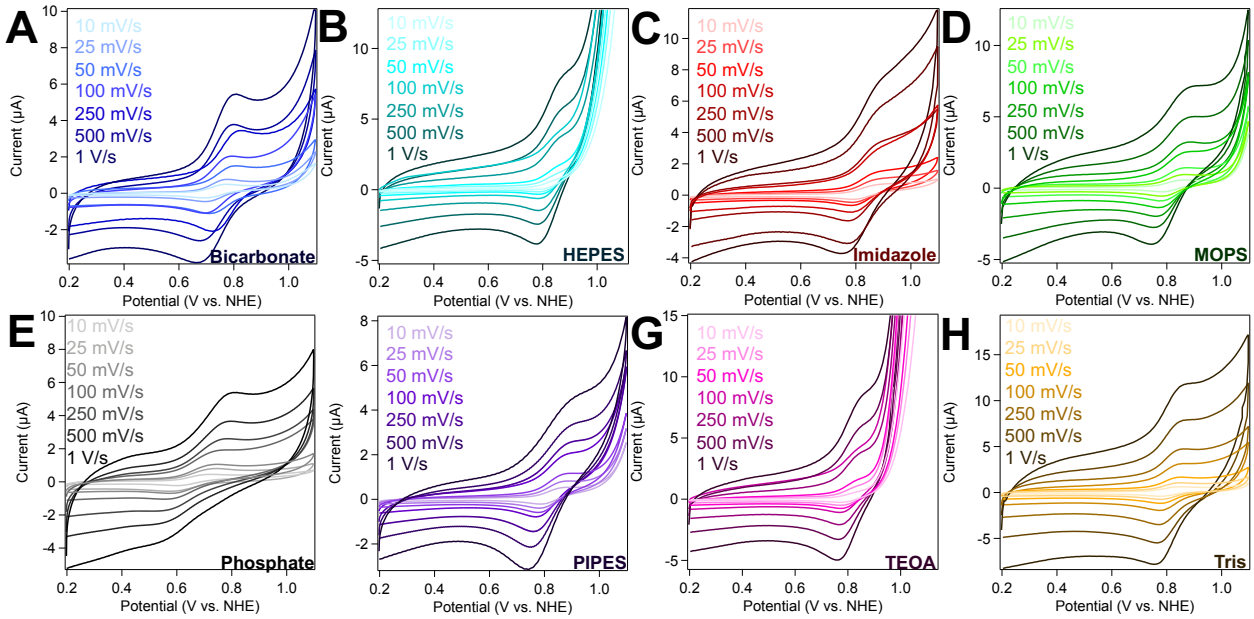

Figure S12. Cyclic voltammograms of $[Ni(cyclam)]^{2+}$ in 100 mM of the indicated buffer under an inert atmosphere at varying scan rates. Samples were collected at the scan rates listed in the figure. All samples contained 100 μM $[Ni(cyclam)]^{2+}$ and 100 mM KCl in 100 mM buffer, pH 7.0. CVs were conducted using a glassy carbon working electrode, Ag/AgCl reference electrode, and a Pt wire counter electrode. Reduction potentials were reported against the normal hydrogen electrode by the addition of +198 mV to the experimentally determined values.

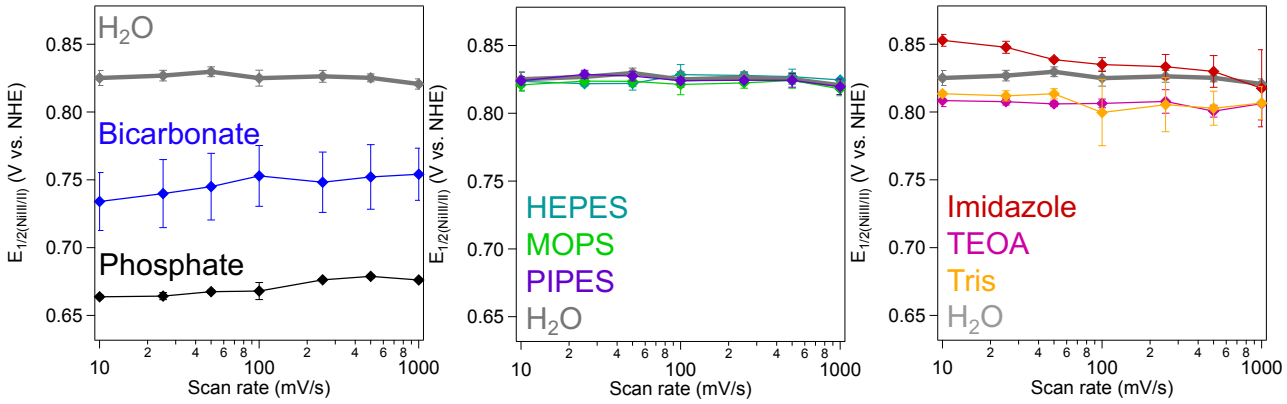

Figure S13. Midpoint [$Ni^{III/II}$(cyclam)] potentials ($E_{1/2}$) as a function of scan rate for each buffer. Cyclic voltammetry was conducted under an inert atmosphere for the buffers indicated in the figure. All reactions contained 100 µM $[Ni(cyclam)]^{2+}$, 100 mM KCl, and 100 mM buffer where appropriate at a final pH of 7.0. CVs were conducted at the following scan rates: 10, 25, 50, 100, 250, 500 and 1000 mV/s. A three-electrode set up was employed with a glassy carbon working electrode, Ag/AgCl reference electrode, and a Pt wire counter electrode. Reduction potentials were reported against the normal hydrogen electrode by the addition of +198 mV to the experimental determined values.

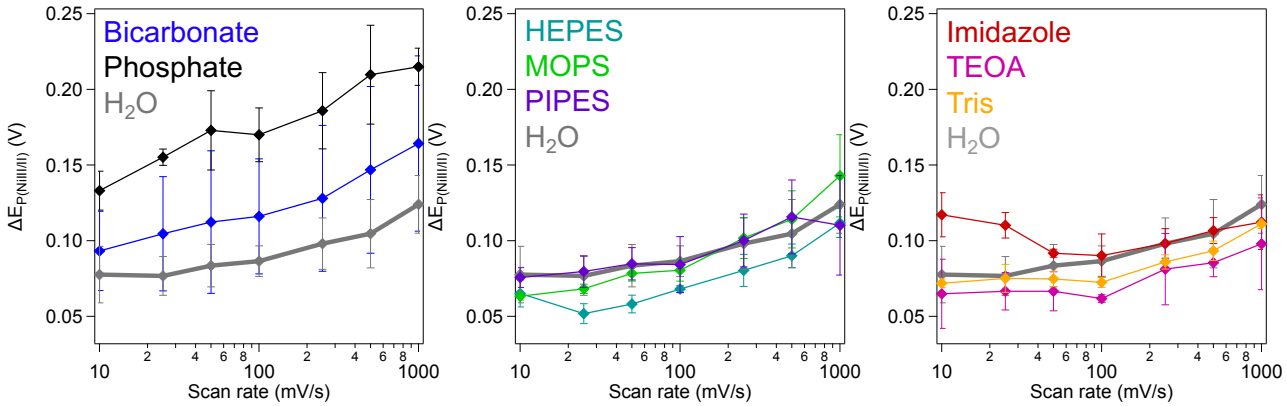

Figure S14. Splitting between [$Ni^{III/II}$(cyclam)] anodic and cathodic peak potentials (ΔE_P) as a function of scan rate in each buffer (as indicated). Cyclic voltammetry was conducted under an inert atmosphere. All samples contained 100 µM $[Ni(cyclam)]^{2+}$, 100 mM KCl, and 100 mM buffer at a final pH of 7.0. CVs were conducted at the following scan rates: 10, 25, 50, 100, 250, 500 and 1000 mV/s. A three-electrode set up was employed using a glassy carbon working electrode, Ag/AgCl reference electrode, and a Pt wire counter electrode. Reduction potentials were reported against the normal hydrogen electrode by the addition of +198 mV to the experimentally determined values.

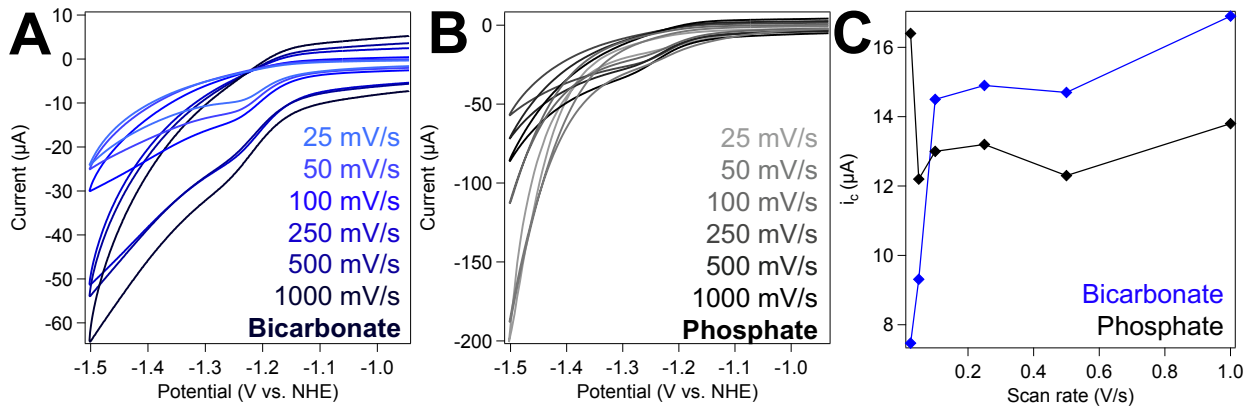

Figure S15. (**A**) and (**B**) Cyclic voltammograms of $[Ni(cyclam)]^{2+}$ and (**C**) catalytic current as a function of scan rate in 100 mM of the indicated anionic buffer under a CO_2-saturating atmosphere at varying scan rates. Samples were collected at the scan rates listed in each panel. All samples contained 100 μM $[Ni(cyclam)]^{2+}$ and 100 mM KCl in 100 mM buffer, pH 7.0. CVs were conducted using a glassy carbon working electrode, Ag/AgCl reference electrode, and a Pt wire counter electrode. Reduction potentials were reported against the normal hydrogen electrode by the addition of +198 mV to the experimentally determined values.

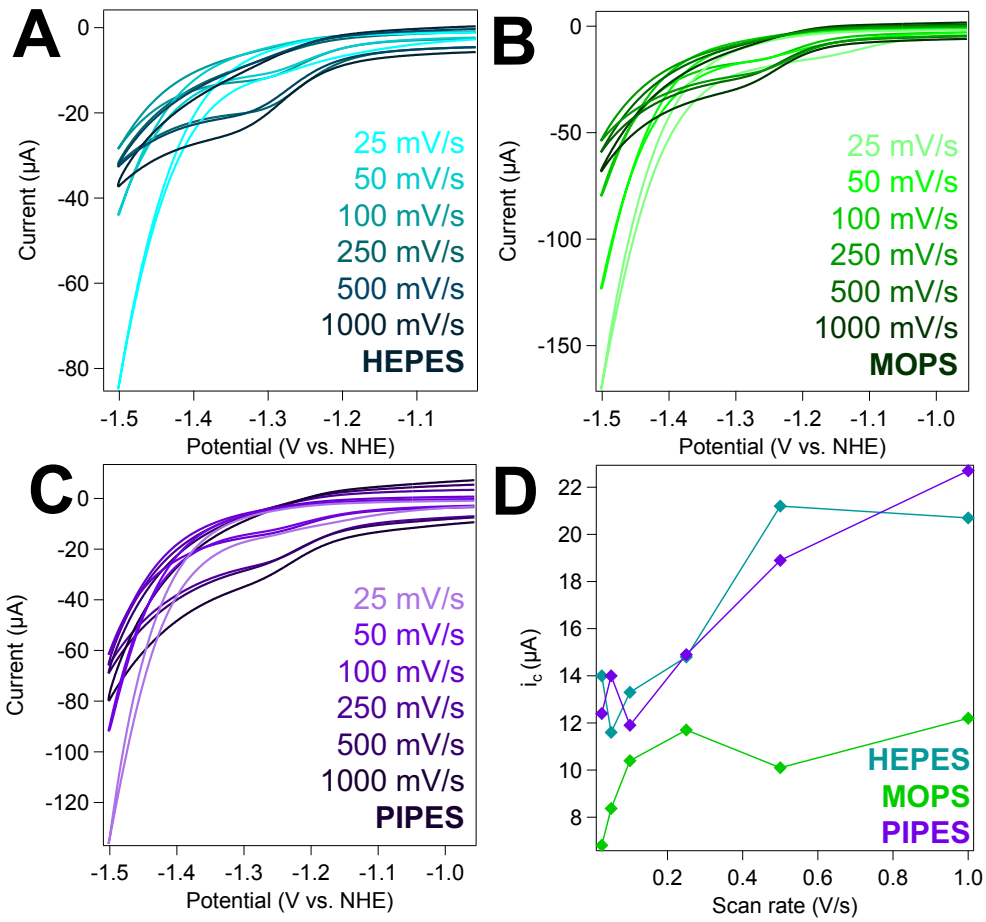

Figure S16. (**A**), (**B**), (**C**) Cyclic voltammograms of $[Ni(cyclam)]^{2+}$ and (**D**) catalytic current as a function of scan rate in 100 mM of the indicated Good's buffer under a CO_2-saturating atmosphere at varying scan rates. Samples were collected at the scan rates listed in each panel. All samples contained 100 μM $[Ni(cyclam)]^{2+}$ and 100 mM KCl in 100 mM buffer, pH 7.0. CVs were conducted using a glassy carbon working electrode, Ag/AgCl reference electrode, and a Pt wire counter electrode. Reduction potentials were reported against the normal hydrogen electrode by the addition of +198 mV to the experimentally determined values.

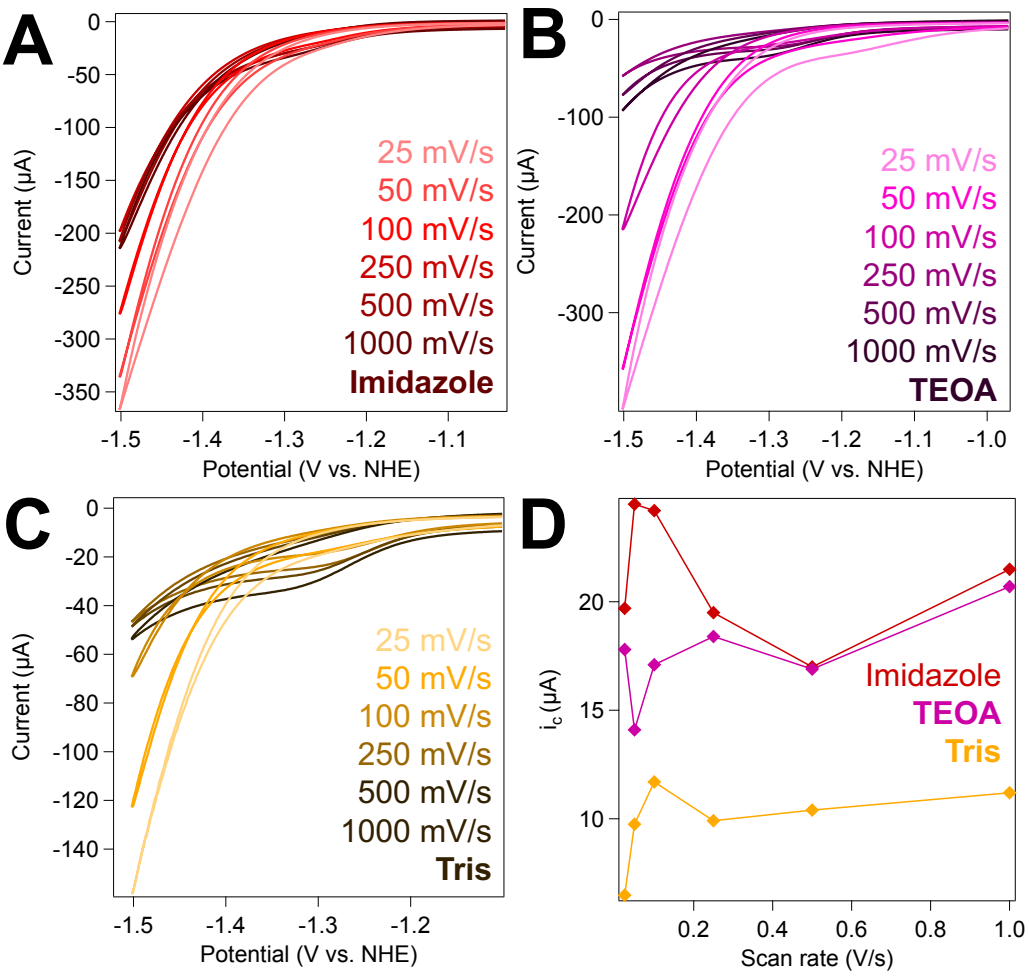

Figure S17. (**A**), (**B**), (**C**) Cyclic voltammograms of $[Ni(cyclam)]^{2+}$ and (**D**) catalytic current as a function of scan rate in 100 mM of the indicated anionic buffer under a CO_2-saturating atmosphere at varying scan rates. Samples were collected at the scan rates listed in each panel. All samples contained 100 μM $[Ni(cyclam)]^{2+}$ and 100 mM KCl in 100 mM buffer, pH 7.0. CVs were conducted using a glassy carbon working electrode, Ag/AgCl reference electrode, and a Pt wire counter electrode. Reduction potentials were reported against the normal hydrogen electrode by the addition of +198 mV to the experimentally determined values.

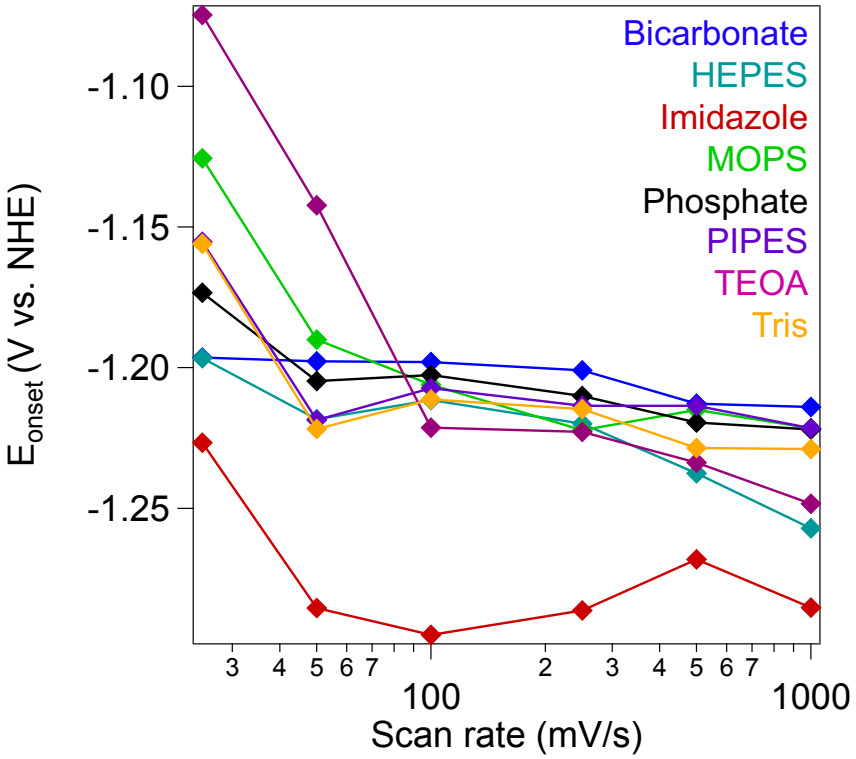

Figure S18. E_{onset} as a function of scan rate. All samples contained 100 μM $[Ni(cyclam)]^{2+}$ and 100 mM KCl in 100 mM buffer, pH 7.0. CVs were conducted under a CO_2-saturating atmosphere using a glassy carbon working electrode, Ag/AgCl reference electrode, and a Pt wire counter electrode. Reduction potentials were reported against the normal hydrogen electrode by the addition of +198 mV to the experimentally determined values.

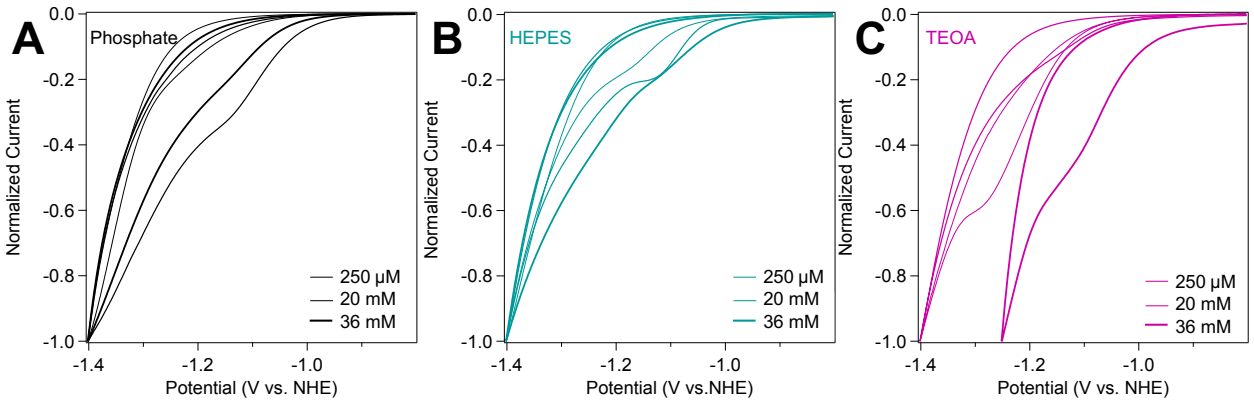

Figure S19. Representative cyclic voltammograms (ν = 50 mV/s) of $[Ni(cyclam)]^{2+}$ in (**A**) phosphate, (**B**) HEPES, and (**C**) TEOA buffers with varying concentrations of CO_2 as indicated. Samples contained 150 µM $[Ni(cyclam)]^{2+}$ and 100 mM KCl in 1 M buffer, pH 7.2. CVs were conducted using a glassy carbon working electrode, Ag/AgCl reference electrode, and a Pt wire counter electrode. Potentials are reported against the normal hydrogen electrode by the addition of +198 mV to the experimentally determined values.

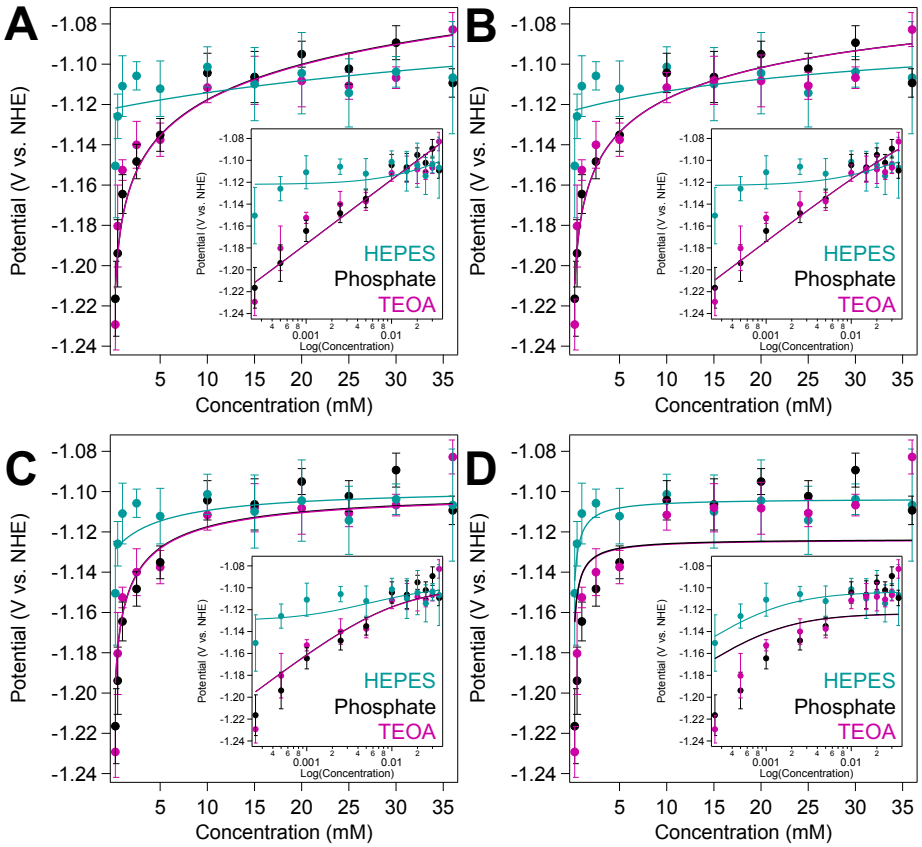

Figure S20. Best-fit traces for CO_2 binding affinity to $[Ni(cyclam)]^+$. Potentials (reported against NHE) were obtained from cyclic voltammograms measured at different CO_2 concentrations (see Figure S19 for representative examples). Samples contained 150 μM $[Ni(cyclam)]^{2+}$ in 1 M buffer with 100 mM KCl, maintained at a pH of 7.2. The data were fit to Eqn 6 with fixed $K_{2,CO2}$ values of (**A**) $K_{2,CO2}$ =1; (**B**) $K_{2,CO2}$ = 10; (**C**) $K_{2,CO2}$ = 100; and (**D**) $K_{2,CO2}$ = 1000 to obtain the best-fit values for $K_{1,CO2}$ and E_{N2} given in Table S1.

Table S1. χ^2 values for the $K_{1,CO2}$ and E_{N2} values presented in Figure S20. Fits selected for main text figure highlighted.

Buffer	Fit Panel	$K_{1,CO2}$ (M^{-1})	$K_{2,CO2}$ (M^{-1})	E_{N2} (V vs. NHE)	χ^2
Phosphate	A	200000	1	-1.511	0.001024
Phosphate	B	300000	10	-1.518	0.000796
Phosphate	C	10000000	100	-1.594	0.001638
Phosphate	D	600000	1000	-1.484	0.008970
TEOA	A	100000	1	-1.501	0.001895
TEOA	B	300000	10	-1.521	0.001615
TEOA	C	300000	100	-1.506	0.001968
TEOA	D	500000	1000	-1.485	0.008263
HEPES	A	40	1	-1.320	0.001456
HEPES	B	60	10	-1.321	0.001399
HEPES	C	400	100	-1.328	0.001078
HEPES	D	200000	1000	-1.441	0.000376

Table S2. Cyclic voltammetry data for the catalytic redox couple of $[Ni(cyclam)]^{2+}$ under CO_2-saturating conditions. Data was collected at the indicated scan rate and all samples contained 100 μM $[Ni(cyclam)]^{2+}$, 100 mM KCl and 100 mM of the indicated anionic buffer, pH 7.0.

Scan rate (mV/s)	**Bicarbonate E_{onset}**	**Bicarbonate i_c (μA)**	**Bicarbonate TOF (s^{-1})**	**Phosphate E_{onset}**	**Phosphate i_c (μA)**	**Phosphate TOF (s^{-1})**
25	-1.20 ± 0.01	-8 ± 2	6	-1.17 ± 0.02	-16 ± 10	25
50	-1.20 ± 0.01	-9 ± 3	8	-1.20 ± 0.01	-12 ± 4	14
100	-1.20 ± 0.01	-15 ± 6	22	-1.20 ± 0.01	-13 ± 3	16
250	-1.20 ± 0.01	-15 ± 5	22	-1.21 ± 0.01	-13 ± 4	16
500	-1.21 ± 0.01	-15 ± 3	22	-1.22 ± 0.02	-12.3 ± 0.4	15
1000	-1.21 ± 0.01	-17 ± 4	28	-1.22 ± 0.02	-13.8 ± 0.1	18

Table S3. Cyclic voltammetry data for the catalytic redox couple of $[Ni(cyclam)]^{2+}$ under CO_2-saturating conditions. Data was collected at the indicated scan rate and all samples contained 100 μM $[Ni(cyclam)]^{2+}$, 100 mM KCl and 100 mM of the indicated Good's buffer, pH 7.0.

Scan rate (mV/s)	**HEPES E_{onset}**	**HEPES i_c (μA)**	**HEPES TOF (s^{-1})**	**MOPS E_{onset}**	**MOPS i_c (μA)**	**MOPS TOF (s^{-1})**	**PIPES E_{onset}**	**PIPES i_c (μA)**	**PIPES TOF (s^{-1})**
25	-1.20 ± 0.05	-14 ± 9	19	-1.13 ± 0.02	-7 ± 3	5	-1.16 ± 0.04	-10 ± 10	10
50	-1.22 ± 0.03	-12 ± 8	14	-1.19 ± 0.04	-8 ± 2	6	-1.22 ± 0.01	-10 ± 10	10
100	-1.21 ± 0.03	-13 ± 9	16	-1.21 ± 0.01	-10 ± 3	10	-1.21 ± 0.01	-12 ± 7	14
250	-1.22 ± 0.03	-15 ± 6	22	-1.22 ± 0.03	-12 ± 4	14	-1.21 ± 0.02	-15 ± 8	22
500	-1.24 ± 0.03	-20 ± 20	38	-1.21 ± 0.02	-10.1 ± 0.1	10	-1.21 ± 0.01	-19 ± 9	35
1000	-1.26 ± 0.04	-20 ± 10	38	-1.22 ± 0.03	-12.2 ± 0.2	14	-1.22 ± 0.01	-23 ± 9	51

Table S4. Cyclic voltammetry data for the catalytic redox couple of $[Ni(cyclam)]^{2+}$ under CO_2-saturating conditions. Data was collected at the indicated scan rate and all samples contained 100 μM $[Ni(cyclam)]^{2+}$, 100 mM KCl and 100 mM of the indicated cationic buffer, pH 7.0.

Scan rate (mV/s)	**Imidazole E_{onset}**	**Imidazole i_c (μA)**	**Imidazole TOF (s^{-1})**	**TEOA E_{onset}**	**TEAO i_c (μA)**	**TEAO TOF (s^{-1})**	**Tris E_{onset}**	**Tris i_c (μA)**	**Tris TOF (s^{-1})**
25	-1.23 ± 0.04	-20 ± 6	38	-1.10 ± 0.02	-20 ± 20	31	-1.16 ± 0.01	-6 ± 4	3
50	-1.29 ± 0.04	-25 ± 2	60	-1.14 ± 0.05	-14 ± 9	19	-1.22 ± 0.03	-10 ± 4	10
100	-1.30 ± 0.03	-24 ± 5	55	-1.22 ± 0.01	-17 ± 5	28	-1.21 ± 0.02	-12 ± 5	14
250	-1.29 ± 0.04	-20 ± 3	38	-1.22 ± 0.01	-18 ± 8	31	-1.21 ± 0.03	-10 ± 3	10
500	-1.27 ± 0.03	-17 ± 3	28	-1.23 ± 0.02	-17 ± 5	28	-1.23 ± 0.04	-10 ± 3	10
1000	-1.29 ± 0.04	-21 ± 4	38	-1.25 ± 0.01	-21 ± 5	42	-1.23 ± 0.05	-11 ± 4	12

Table S5. Product formation by $[Ni(cyclam)]^{2+}$ following 2.5 hours of irradiation. Samples contained 10 μM $[Ni(cyclam)]^{2+}$, 1 mM $[Ru(bpy)_3]^{2+}$, and 100 mM ascorbate in 1 M buffer, pH 7.0. Assays were conducted under a saturating carbon dioxide atmosphere at 4 °C. Values reported are the average and standard deviation of at least three independent trials. All values were corrected for baseline activity by subtracting any CO or H_2 produced by the corresponding control of 1 mM $[Ru(bpy)_3]^{2+}$ and 100 mM ascorbate in 1 M buffer control assays.

Buffer	CO (nmole)	CO TON	H_2 (nmole)	H_2 TON	% CO selective
Bicarbonate	310 ± 20	10.2 ± 0.7	7 ± 4	0.2 ± 0.8	98 ± 5
HEPES	47 ± 17	1.6 ± 0.6	23 ± 17	0.8 ± 0.5	67 ± 9
Imidazole	2700 ± 600	90 ± 20	ND[a]	ND	100[b]
MOPS	18 ± 4	0.6 ± 0.1	ND	ND	100
Phosphate	390 ± 60	13 ± 2	1300 ± 400	40 ± 10	23 ± 4
PIPES	44 ± 9	1.5 ± 0.3	130 ± 70	4 ± 2	30 ± 10
TEOA	30 ± 9	1.0 ± 0.3	ND	ND	100
Tris	250 ± 98	8 ± 3	ND	ND	100

[a] ND = not detected

[b] Buffers reported to be 100% selective produced no hydrogen above the control samples.

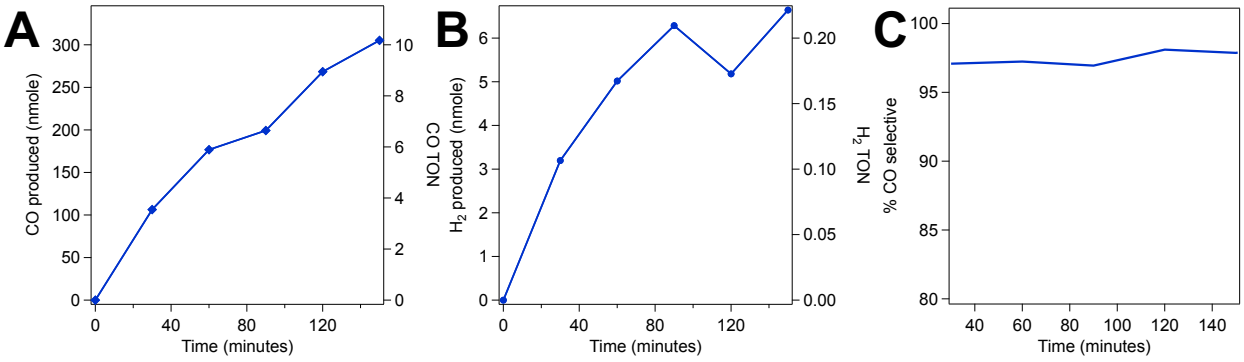

Figure S21. Photoassay product distribution by $[Ni(cyclam)]^{2+}$ in sodium bicarbonate buffer. (**A**) CO production; (**B**) H_2 production; (**C**) Selectivity as indicated by % CO selective, as described in Section 2.5 using Equation 8. Samples contained 10 µM $[Ni(cyclam)]^{2+}$, 1 mM $[Ru(bpy)_3]^{2+}$, and 100 mM ascorbate in 1 M buffer, pH 7.0. Assays were conducted under a saturating carbon dioxide atmosphere. Samples were irradiated using 447.5 nm LEDs at 4 °C. All values were corrected for baseline levels by subtracting any CO or H_2 produced by the corresponding control of 1 mM $[Ru(bpy)_3]^{2+}$ with 100 mM ascorbate in 1 M bicarbonate.

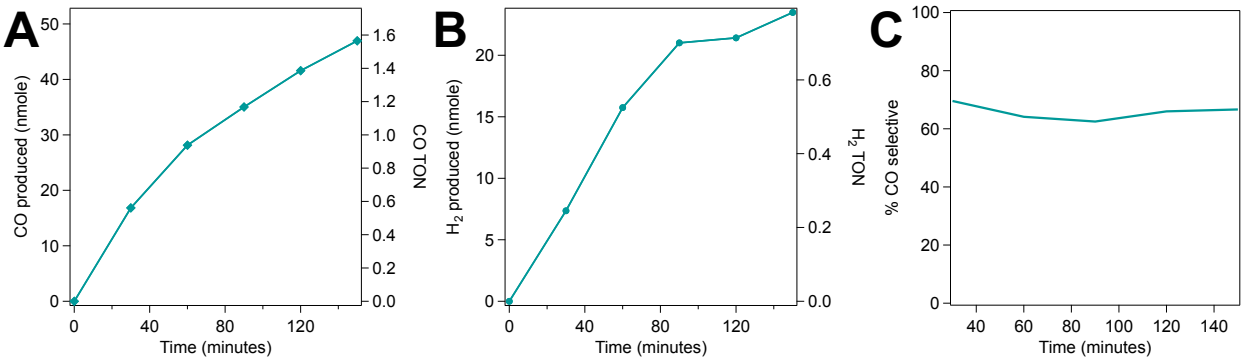

Figure S22. Photoassay product distribution by $[Ni(cyclam)]^{2+}$ in HEPES buffer. (**A**) CO production; (**B**) H_2 production; (**C**) Selectivity as indicated by % CO selective, as described in Section 2.5 using Equation 8. Samples contained 10 µM $[Ni(cyclam)]^{2+}$, 1 mM $[Ru(bpy)_3]^{2+}$, and 100 mM ascorbate in 1 M buffer, pH 7.0. Assays were conducted under a saturating carbon dioxide atmosphere. Samples were irradiated using 447.5 nm LEDs at 4 °C. All values were corrected for baseline levels by subtracting any CO or H_2 produced by the corresponding control of 1 mM $[Ru(bpy)_3]^{2+}$ with 100 mM ascorbate in 1 M HEPES.

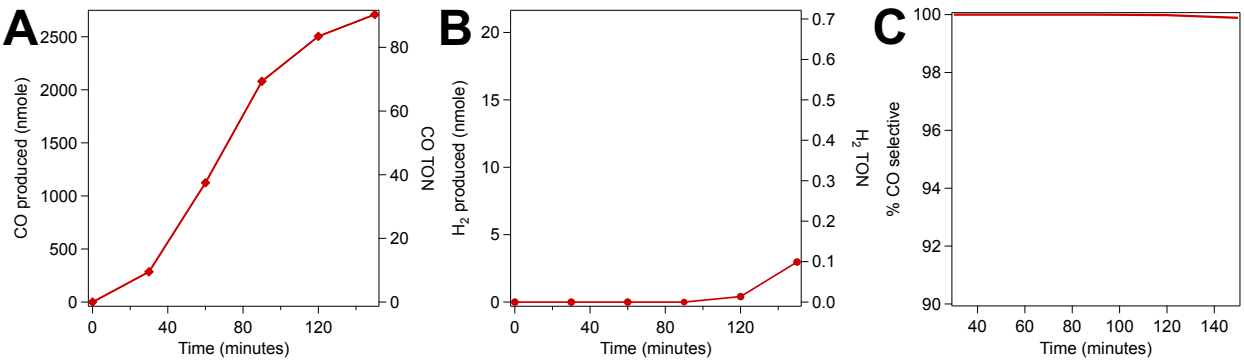

Figure S23. Photoassay product distribution by $[Ni(cyclam)]^{2+}$ in imidazole buffer. (**A**) CO production; (**B**) H_2 production; (**C**) Selectivity as indicated by % CO selective, as described in Section 2.5 using Equation 8. Samples contained 10 µM $[Ni(cyclam)]^{2+}$, 1 mM $[Ru(bpy)_3]^{2+}$, and 100 mM ascorbate in 1 M buffer, pH 7.0. Assays were conducted under a saturating carbon dioxide atmosphere. Samples were irradiated using 447.5 nm LEDs at 4 °C. All values were corrected for baseline levels by subtracting any CO or H_2 produced by the corresponding control of 1 mM $[Ru(bpy)_3]^{2+}$ with 100 mM ascorbate in 1 M imidazole.

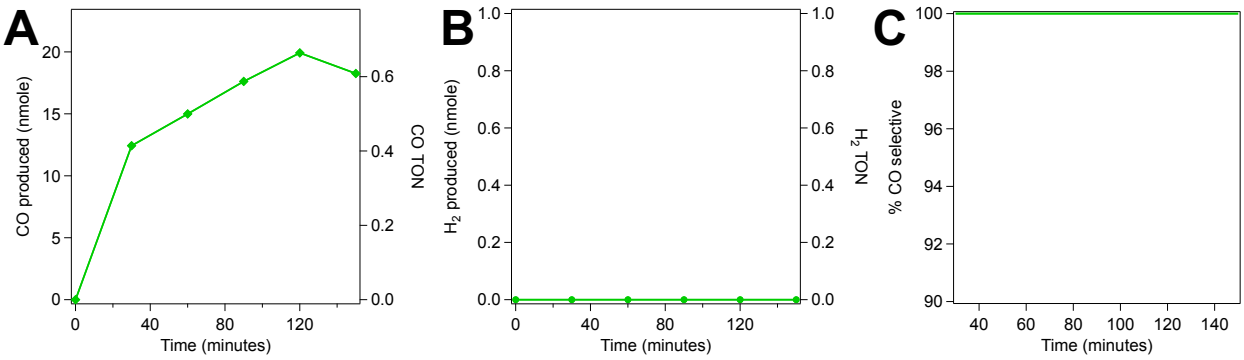

Figure S24. Photoassay product distribution by $[Ni(cyclam)]^{2+}$ in MOPS buffer. (**A**) CO production; (**B**) H_2 production; (**C**) Selectivity as indicated by % CO selective, as described in Section 2.5 using Equation 8. Samples contained 10 µM $[Ni(cyclam)]^{2+}$, 1 mM $[Ru(bpy)_3]^{2+}$, and 100 mM ascorbate in 1 M buffer, pH 7.0. Assays were conducted under saturating carbon dioxide atmospheres. Samples were irradiated using 447.5 nm LEDs at 4 °C. All values were corrected for baseline levels by subtracting any CO or H_2 produced by the corresponding control of 1 mM $[Ru(bpy)_3]^{2+}$ with 100 mM ascorbate in 1 M MOPS.

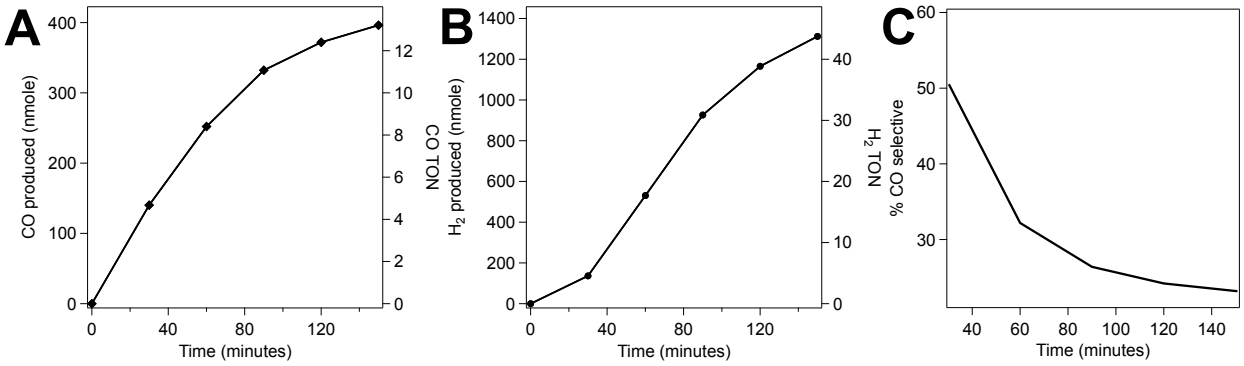

Figure S25. Photoassay product distribution by $[Ni(cyclam)]^{2+}$ in phosphate buffer. (**A**) CO production; (**B**) H_2 production; (**C**) Selectivity as indicated by % CO selective, as described in Section 2.5 using Equation 8. Samples contained 10 μM $[Ni(cyclam)]^{2+}$, 1 mM $[Ru(bpy)_3]^{2+}$, and 100 mM ascorbate in 1 M buffer, pH 7.0. Assays were conducted under saturating carbon dioxide atmospheres. Samples were irradiated using 447.5 nm LEDs at 4 °C. All values were corrected for baseline levels by subtracting any CO or H_2 produced by the corresponding control of 1 mM $[Ru(bpy)_3]^{2+}$ with 100 mM ascorbate in 1 M phosphate.

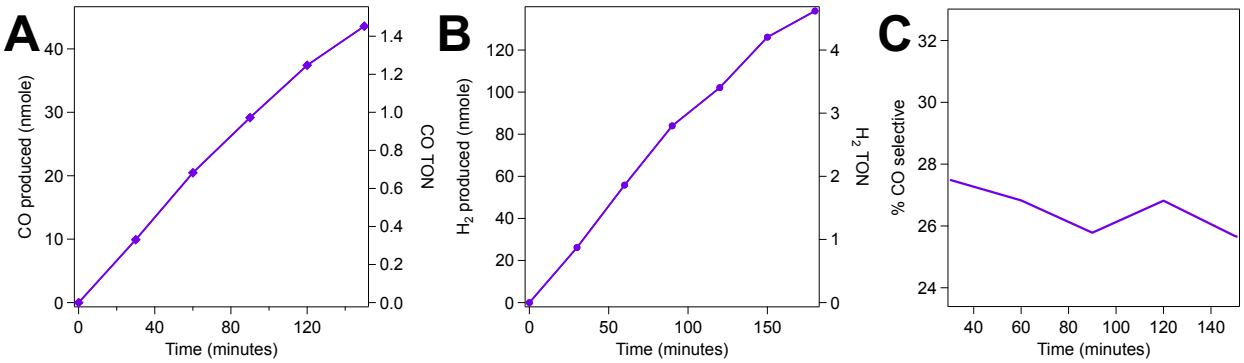

Figure S26. Photoassay product distribution by $[Ni(cyclam)]^{2+}$ in PIPES buffer. (**A**) CO production; (**B**) H_2 production; (**C**) Selectivity as indicated by % CO selective, as described in Section 2.5 using Equation 8. Samples contained 10 µM $[Ni(cyclam)]^{2+}$, 1 mM $[Ru(bpy)_3]^{2+}$, and 100 mM ascorbate in 1 M buffer, pH 7.0. Assays were conducted under saturating carbon dioxide atmospheres. Samples were irradiated using 447.5 nm LEDs at 4 °C. All values were corrected for baseline levels by subtracting any CO or H_2 produced by the corresponding control of 1 mM $[Ru(bpy)_3]^{2+}$ with 100 mM ascorbate in 1 M PIPES.

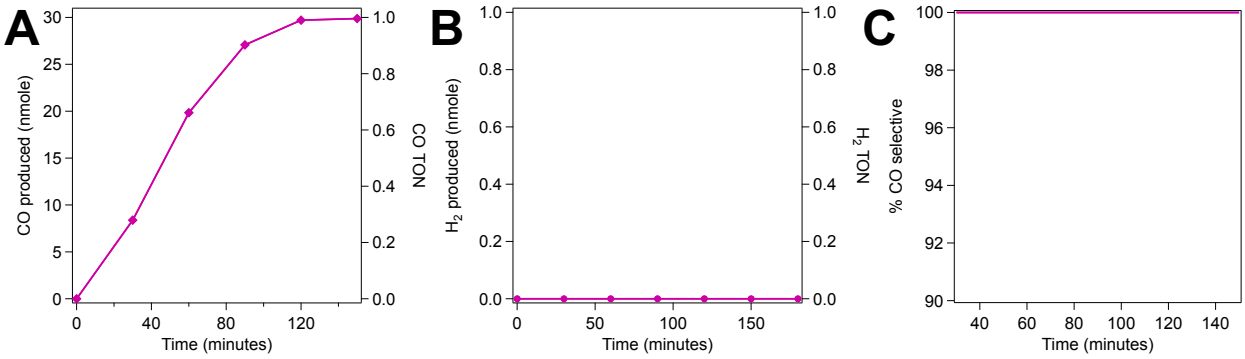

Figure S27. Photoassay product distribution by $[Ni(cyclam)]^{2+}$ in TEOA buffer. (**A**) CO production; (**B**) H_2 production; (**C**) Selectivity as indicated by % CO selective, as described in Section 2.5 using Equation 8. Samples contained 10 µM $[Ni(cyclam)]^{2+}$, 1 mM $[Ru(bpy)_3]^{2+}$, and 100 mM ascorbate in 1 M buffer, pH 7.0. Assays were conducted under saturating carbon dioxide atmospheres. Samples were irradiated using 447.5 nm LEDs at 4 °C. All values were corrected for baseline levels by subtracting any CO or H_2 produced by the corresponding control of 1 mM $[Ru(bpy)_3]^{2+}$ with 100 mM ascorbate in 1 M TEOA.

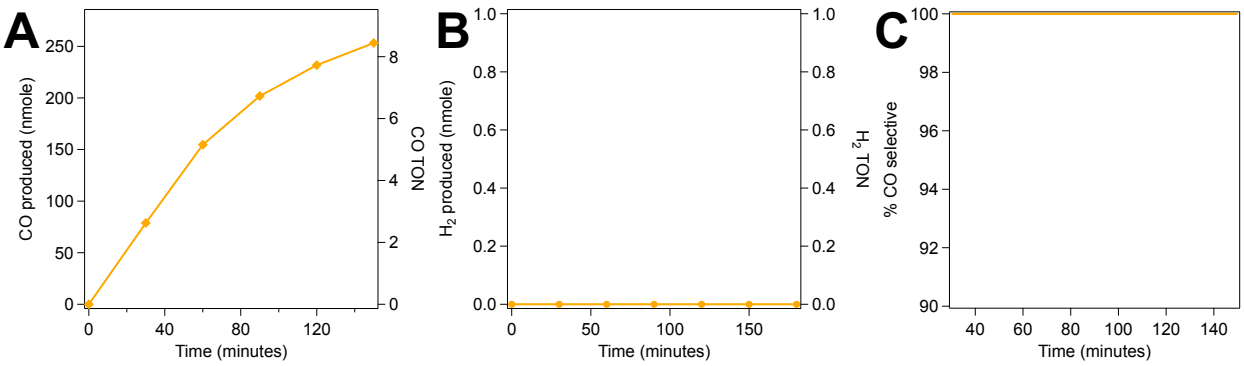

Figure S28. Photoassay product distribution by $[Ni(cyclam)]^{2+}$ in Tris buffer. (**A**) CO production; (**B**) H_2 production; (**C**) Selectivity as indicated by % CO selective, as described in Section 2.5 using Equation 8. Samples contained 10 µM $[Ni(cyclam)]^{2+}$, 1 mM $[Ru(bpy)_3]^{2+}$, and 100 mM ascorbate in 1 M buffer, pH 7.0. Assays were conducted under saturating carbon dioxide atmospheres. Samples were irradiated using 447.5 nm LEDs at 4 °C. All values were corrected for baseline levels by subtracting any CO or H_2 produced by the corresponding control of 1 mM $[Ru(bpy)_3]^{2+}$ with 100 mM ascorbate in 1 M Tris.

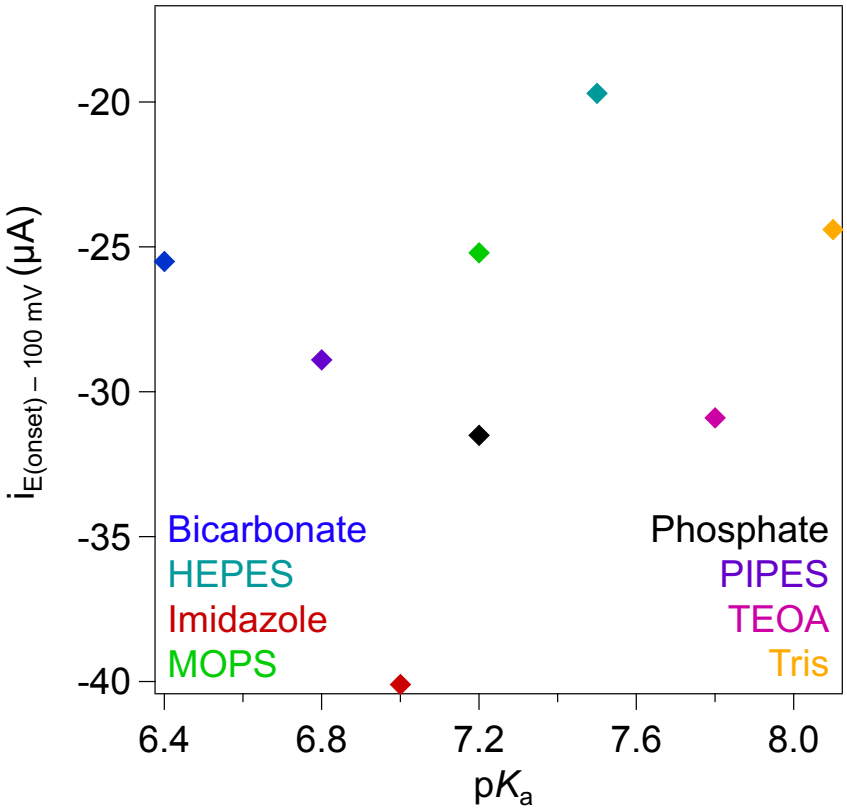

Figure S29. Current as a function of pK_a. Current was determined as the current at the onset potential determined for each buffer - 100 mV. All samples contained 100 μM $[Ni(cyclam)]^{2+}$, 100 mM KCl, and 100 mM buffer at a final pH of 7.0 under a saturating CO_2 atmosphere. CVs were conducted at a scan rate of 1 V/s using a glassy carbon working electrode, Ag/AgCl reference electrode, and a Pt wire counter electrode.

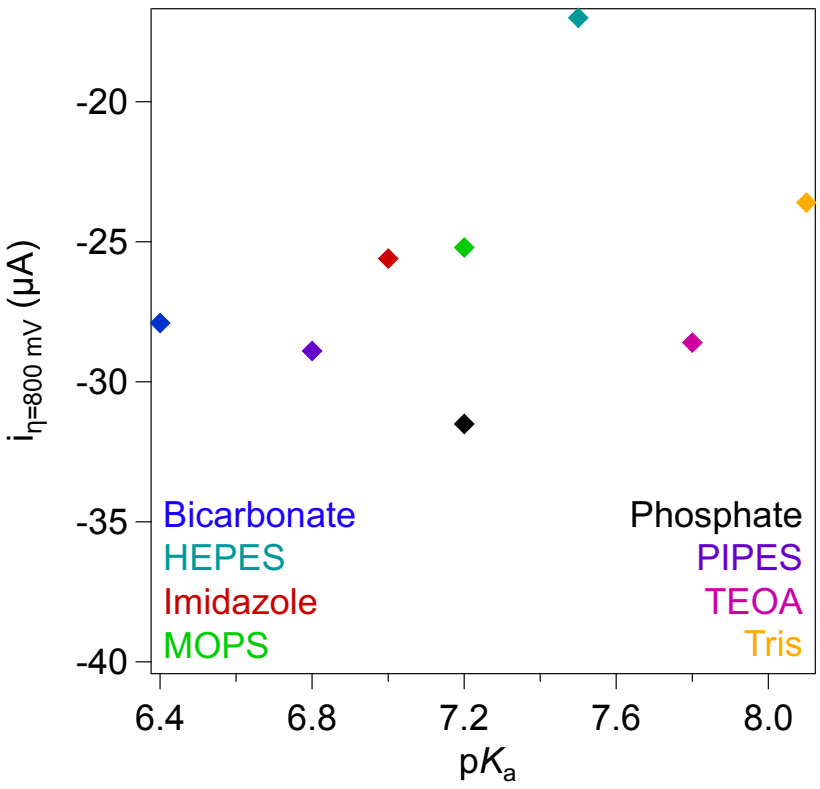

Figure S30. Current as a function of pK_a. Current was determined as the current at a constant overpotential of 800 mV compared to the CO_2/CO reduction potential of – 520 mV vs. NHE. All samples contained 100 μM $[Ni(cyclam)]^{2+}$, 100 mM KCl, and 100 mM buffer at a final pH of 7.0 under a saturating CO_2 atmosphere. CVs were conducted at a scan rate of 1 V/s using a glassy carbon working electrode, Ag/AgCl reference electrode, and a Pt wire counter electrode.